Spectroscopic investigation of light strange $S = -1$ Λ and Σ and $S = -2$ Ξ baryons

Chandni Menapara† Ajay Kumar Rai

Department of Physics, Sardar Vallabhbhai National Institute of Technology, Surat- 395007, Gujarat, India

Abstract: The present study is dedicated to light-strange Λ with strangeness $S = -1$ and isospin $I = 0$, Σ with $S = -1$ and $I = 1$, and Ξ baryon with $S = -2$ and $I = \frac{1}{2}$. In this study, the hypercentral constituent quark model with linear confining potential has been employed along with a first order correction term to obtain the resonance masses up to approximately 4 GeV. The calculated states include 1*S*-5*S*, 1*P*-4*P*, 1*D*-3*D*, 1*F*-2*F*, and 1*G* (in a few cases) along with all possible spin-parity assignments. Regge trajectories have been explored for the linearity of the calculated masses for (n, M^2) and (J, M^2). Magnetic moments have been intensively studied for ground state spin $\frac{1}{2}$ and $\frac{3}{2}$, in addition to the configuration mixing of the first negative parity state for Ξ. Lastly, the transition magnetic moments and radiative decay widths have been presented.

Keywords: mass spectra, strange baryon, Regge trajectory, magnetic moment

DOI: 10.1088/1674-1137/abf4f4

I. INTRODUCTION

The objective of the study of hadrons is to reveal the possible degrees of freedom responsible for the appearance of a given system. The quark confinement and asymptotic freedom have been the starting points of any theoretical and phenomenological study to understand quark dynamics. Hadron spectroscopy attempts to explore the excited mass spectrum along with the multiplet structure and spin-parity assignments. The light quark baryons form the basis of octets and decuplets ranging from strangeness $S = 0$ to $S = -3$ based on symmetric, asymmetric, and mixed-symmetric flavor-spin combinations.

$$3 \otimes 3 \otimes 3 = 1^A \oplus 8^M \oplus 8^M \oplus 10^S .$$

The presence of a strange quark in a baryon draws attention because it would be slightly heavier than u and d quarks and considerably lighter than c and b quarks. Particularly, the strangeness $S = -2$ Ξ baryons have not been observed experimentally like other light sector baryons [1], as depicted in Table 1. The limited observations in the Ξ baryon group are owing to the fact that they are produced only as the final state in a process in addition to having considerably small cross-sections [2]. Unlike the Ξ baryons, Σ and Λ with $S = -1$ have quite a number of experimentally established states.

The present article is dedicated to the study of Λ, Σ and Ξ baryons. Cascade baryons appear with isospin $I = \frac{1}{2}$ in the octet ($J = \frac{1}{2}$) and decuplet ($J = \frac{3}{2}$) as Ξ and Ξ^*, respectively. The quark combination is uss for Ξ^0 and dss for Ξ^-.

For mixed symmetry flavor wave-function in the octet group,

$$\begin{aligned}
\Xi^0 \rightarrow &\quad \frac{1}{\sqrt{6}}(sus + uss - 2ssu),\\
\Xi^- \rightarrow &\quad \frac{1}{\sqrt{6}}(dss + sds - 2ssd),\\
\Xi^0 \rightarrow &\quad \frac{1}{\sqrt{2}}(uss - sus),\\
\Xi^- \rightarrow &\quad \frac{1}{\sqrt{2}}(dss - sds).
\end{aligned}$$

For symmetric flavor wave-function in the decuplet group,

$$\begin{aligned}
\Xi^{*0} \rightarrow &\quad \frac{1}{\sqrt{3}}(uss + sus + ssu),\\
\Xi^{*-} \rightarrow &\quad \frac{1}{\sqrt{3}}(dss + sds + ssd).
\end{aligned}$$

Received 10 February 2021; Accepted 6 April 2021; Published online 17 May 2021

† E-mail: chandni.menapara@gmail.com

Table 1. Ξ listed by Particle Data Group (PDG [1]).

State	J^P	Status
$\Xi^0(1314)$	$\frac{1}{2}^+$	****
$\Xi^-(1321)$	$\frac{1}{2}^+$	****
Ξ(1530)	$\frac{3}{2}^+$	****
Ξ(1620)		*
Ξ(1690)		***
Ξ(1820)	$\frac{3}{2}^-$	***
Ξ(1950)		***
Ξ(2030)	$\frac{5}{2}^?$	***
Ξ(2120)		*
Ξ(2250)		**
Ξ(2370)		**
Ξ(2500)		*

Similarly, the Σ baryon with u, d, and s constituent quarks has a place in octets and decuplets with three possible combinations as uus, uds, and dds respectively. The Λ baryon appearing in an octet as $I = 0$ has uds quark content; however, its wave-function differs from that of Σ^0.

Experimental facilities around the world have been striving to study strange hyperons. A recent study at CERN by ALICE Collaboration established an attractive interaction between protons and Ξ^- [3]. Activities in measuring weak decays of Ξ hyperons were reported by the KTeV Collaboration [4] and the NA48/1 Collaboration [5]; the BABAR Collaboration has also been carrying out extensive studies [6]. The photoproduction of Ξ has been observed by CLAS detector at Jefferson Lab [7]. Additionally, JLab has recently proposed to explore the strange hyperon spectroscopy through a secondary KL beam along with a GlueX experiment [8], and the findings are expected to provide new direction and understanding of strange hyperons Σ, Λ, and Ξ. The BESIII Collaboration observed Ξ(1530) in a baryon-antibaryon pair from charmonium decay [9]. The upcoming experimental facility PANDA at FAIR-GSI has high expectations to establish the whole spectrum of hyperons through proton-antiproton collisions [10-13]. A Ξ dedicated study has been undertaken for mass, width, and decay modes by a member of the PANDA group [14-16].

In the case of Σ and Λ baryons, all properties are not completely known. Most of the data for strange baryons have been based on earlier studies from a bubble chamber for K^- reactions. The Λ(1405) with $J^P = \frac{1}{2}^-$ is still a mysterious state in the lambda spectrum. This state is lower than the non-strange counterpart $N^*(1535)$. Recent studies have attempted to understand this state as hadronic molecular [17, 18]. The JPAC and Osaka-ANL groups have applied a coupled channel approach to study these dynamics [19, 20]. Additionally, a two pole structure of Λ(1405) has been analyzed using chiral effective field theory [21]. E. Klempt *et al.* has extensively reviewed the Λ and Σ hyperon spectrum based on experimental and theoretical studies focusing on all the known states of the spectrum [22]. These spectra are studied through photoproduction off the proton in ref. [23]. The study of strangeness $S = -1$ and -2 becomes more interesting not only in a high energy arena but also in astrophysical bodies such as neutron stars [24].

The excited states of hyperons have been investigated using phenomenological as well as theoretical approaches. Various models have attempted to reproduce the octet and decuplet ground states and a range of excited states. A recent review has summarized in detail a few strange baryon spectrum states with theoretical and experimental aspects [25]. L. Xiao *et al*. intensively studied the strong decays of Ξ under the chiral quark model, which may assist in determining the possible spin-parity of a given state in strong decay [26]. Some of the models have been summarized briefly in Sec. 3, ranging from the relativistic approach [27], instanton induced model [28], CI model [29], algebraic model [30], and Skyrme model [31], etc. The present work is based on the phenomenological non-relativistic hypercentral constituent quark model [32]. Similar studies have previously been carried out for nucleons and delta baryons, which serve as guides towards exploring strange baryons [33-36].

This paper is organized as follows: after the briefing on hadron spectroscopy and various experimental and theoretical approaches, Sec. 2 deals with the background of the model used. Sec. 3 describes the results for resonance masses and provides a detailed discussion regarding the data presented in respective tables. Sec. 4 presents the Regge trajectories and deductions based on them. Sec. 5 is dedicated to the magnetic moments of the isospin states of Ξ, Σ, and Λ based on their effective masses. Sec. 6 focuses on the transition magnetic moments and radiative decay widths, and lastly, the conclusion ends the paper.

II. THEORETICAL BACKGROUND

The constituent quark model (CQM) is based on a simple assumption of baryon as a system of three quarks (or anti-quarks) interacting by some potential, which ultimately may provide a quantitative description of baryonic properties. It is obvious that the QCD quark masses are considerably smaller than constituent quark masses; however, this large mass parametrizes all the other effects in a baryon. Thus, the CQMs have been employed in various studies through various modifications in non-relativistic or semi-relativistic approaches.

The hypercentral constituent quark model (hCQM) has been employed for the present study, which is a non relativistic approach [37, 38]. It undertakes the baryon as a confined system of three quarks wherein the potential is hypercentral one. The dynamics of a three body system are addressed using the Jacobi coordinates, introduced as ρ and λ, reducing the body parameters to two [39].

$$\rho = \frac{1}{\sqrt{2}}(\boldsymbol{r_1} - \boldsymbol{r_2}), \tag{1}$$

$$\lambda = \frac{(m_1\boldsymbol{r_1} + m_2\boldsymbol{r_2} - (m_1+m_2)\boldsymbol{r_3})}{\sqrt{m_1^2 + m_2^2 + (m_1+m_2)^2}}. \tag{2}$$

The hyperradius and hyperangle are defined as

$$x = \sqrt{\rho^2 + \lambda^2}; \quad \xi = \arctan\left(\frac{\rho}{\lambda}\right). \tag{3}$$

The Hamiltonian of the system is written with the potential term solely depending on the hyperradius x of the three body system

$$H = \frac{P^2}{2m} + V^0(x) + V_{\rm SD}(x), \tag{4}$$

where $m = \dfrac{2m_\rho m_\lambda}{m_\rho + m_\lambda}$ is the reduced mass. Thus the hyperradial part of the wave-function as determined by the hypercentral Schrodinger equation is [40]

$$\left[\frac{{\rm d}^2}{{\rm d}x^2} + \frac{5}{x}\frac{\rm d}{{\rm d}x} - \frac{\gamma(\gamma+4)}{x^2}\right]\psi(x) = -2m[E - V(x)]\psi(x). \tag{5}$$

Here, γ replaces the angular momentum quantum number with the relation $l(l+1) \to \dfrac{15}{4} + \gamma(\gamma+4)$. The choice of hypercentral potential narrows down to a hyperCoulomb one, i.e., $-\dfrac{\tau}{x}$. The confinement term here is chosen to be of linear nature.

$$V^0(x) = -\frac{\tau}{x} + \alpha x. \tag{6}$$

Here, $\tau = \dfrac{2}{3}\alpha_s$, with α_s being a running coupling constant and α a parameter based on the fitting of the ground state for a given system.

The $V_{\rm SD}(x)$ accounts for the spin-dependent terms leading to hyperfine interactions.

$$V_{SD}(x) = V_{SS}(x)(\boldsymbol{S}_\rho \cdot \boldsymbol{S}_\lambda) + V_{\gamma S}(x)(\gamma \cdot \boldsymbol{S}) + V_T \times \left[S^2 - \frac{3(\boldsymbol{S}\cdot\boldsymbol{x})(\boldsymbol{S}\cdot\boldsymbol{x})}{x^2}\right]. \tag{7}$$

where $V_{SS}(x)$, $V_{\gamma S}(x)$, and $V_T(x)$ are spin-spin, spin-orbit, and tensor terms, respectively [41]. In the present study, a first order correction term to the potential with $\dfrac{1}{m}$ dependence has also been added as $\dfrac{1}{m}V^1(x)$ [42-44].

$$V^1(x) = -C_F C_A \frac{\alpha_s^2}{4x^2}, \tag{8}$$

where C_F and C_A are Casimir elements of fundamental and adjoint representation.

The resonance masses have been obtained with and without the first order correction term. The constituent quark masses have been taken to be $m_u = m_d = 0.290$ MeV and $m_s = 0.500$ MeV. Mathematica Notebook has been employed for numerical solutions [45].

III. RESULTS AND DISCUSSION FOR THE RESONANCE MASS SPECTRA

In the present work, the resonance masses are calculated for radial and orbital states from 1*S*-5*S*, 1*P*-4*P*, 1*D*-3*D*, and 1*F*-2*F*. In Tables 2-20, the resonance mass for all the possible spin-parity configurations for each state with $S = \dfrac{1}{2}$ and $S = \dfrac{3}{2}$ has been considered and the respective contribution has been calculated based on the model discussed in Sec. 2, including with and without first order corrections. For *S*-state, possible total angular momentum and parity are $\dfrac{1}{2}^+$ and $\dfrac{3}{2}^+$ (Tables 2, 8, and 15); for *P*-state, the range goes from $\dfrac{1}{2}^-$ to $\dfrac{5}{2}^-$ (Tables 3, 9, and 16); for *D*-state, the range is $\dfrac{3}{2}^+$ to $\dfrac{7}{2}^+$ (Tables 4, 10, and 17); and for *F*-state, it is $\dfrac{3}{2}^-$ to $\dfrac{9}{2}^-$ (Tables 5, 11, and 18). Additionally, for *G*-state, the range is from $\dfrac{5}{2}^+$ to $\dfrac{11}{2}^+$ (Table 12) (only calculated for baryon). Only a few experimentally established states with four star status availability are mentioned in their respective tables. In the tables, $Mass_{\rm cal}1$ and $Mass_{\rm cal}2$ represent resonance masses without and with first order correction, respectively, in MeV.

An attempt has been made to summarize the calculated masses in this paper along with those of different models.Tables 6, 7, 13, 14, 19, and 20 depict the range of masses for a given J^P value irrespective of the assigned state in increasing order. It is evident that the low lying resonance states are within a reasonable range for almost all of the models and approaches listed. However, the higher states have huge variations possibly because of the fact that not a single model exactly predicts the spin-parity assignments, and in addition, there is no experimental

Table 2. *S*-wave of Ξ baryon (in MeV).

State	J^P	$Mass_{\rm cal}1$	$Mass_{\rm cal}2$	$Mass_{\rm exp}$ [1]
$1S$	$\frac{1}{2}^+$	1322	1321	1321
	$\frac{3}{2}^+$	1531	1524	1532
$2S$	$\frac{1}{2}^+$	1884	1891	
	$\frac{3}{2}^+$	1971	1964	
$3S$	$\frac{1}{2}^+$	2361	2372	
	$\frac{3}{2}^+$	2457	2459	
$4S$	$\frac{1}{2}^+$	2935	2954	
	$\frac{3}{2}^+$	3029	3041	
$5S$	$\frac{1}{2}^+$	3591	3620	
	$\frac{3}{2}^+$	3679	3702	

Table 3. *P*-wave of Ξ baryon (in MeV).

State	J^P	$Mass_{\rm cal}1$	$Mass_{\rm cal}2$	$Mass_{\rm exp}$ [1]
$1^2P_{1/2}$	$\frac{1}{2}^-$	1886	1889	
$1^2P_{3/2}$	$\frac{3}{2}^-$	1871	1873	1823
$1^4P_{1/2}$	$\frac{1}{2}^-$	1894	1897	
$1^4P_{3/2}$	$\frac{3}{2}^-$	1879	1881	1823
$1^4P_{5/2}$	$\frac{5}{2}^-$	1859	1859	
$2^2P_{1/2}$	$\frac{1}{2}^-$	2361	2373	
$2^2P_{3/2}$	$\frac{3}{2}^-$	2337	2347	
$2^4P_{1/2}$	$\frac{1}{2}^-$	2373	2386	
$2^4P_{3/2}$	$\frac{3}{2}^-$	2349	2360	
$2^4P_{5/2}$	$\frac{5}{2}^-$	2318	2325	
$3^2P_{1/2}$	$\frac{1}{2}^-$	2929	2948	
$3^2P_{3/2}$	$\frac{3}{2}^-$	2894	2913	
$3^4P_{1/2}$	$\frac{1}{2}^-$	2946	2966	
$3^4P_{3/2}$	$\frac{3}{2}^-$	2912	2931	
$3^4P_{5/2}$	$\frac{5}{2}^-$	2865	2884	
$4^2P_{1/2}$	$\frac{1}{2}^-$	3577	3609	
$4^2P_{3/2}$	$\frac{3}{2}^-$	3532	3563	
$4^4P_{1/2}$	$\frac{1}{2}^-$	3599	3632	
$4^4P_{3/2}$	$\frac{3}{2}^-$	3554	3586	
$4^4P_{5/2}$	$\frac{5}{2}^-$	3494	3524	

Table 4. *D*-wave of Ξ baryon (in MeV).

State	J^P	$Mass_{\rm cal}1$	$Mass_{\rm cal}2$	$Mass_{\rm exp}$ [1]
$1^2D_{3/2}$	$\frac{3}{2}^+$	2270	2281	
$1^2D_{5/2}$	$\frac{5}{2}^+$	2234	2244	
$1^4D_{1/2}$	$\frac{1}{2}^+$	2310	2322	
$1^4D_{3/2}$	$\frac{3}{2}^+$	2283	2295	
$1^4D_{5/2}$	$\frac{5}{2}^+$	2247	2257	
$1^4D_{7/2}$	$\frac{7}{2}^+$	2203	2211	
$2^2D_{3/2}$	$\frac{3}{2}^+$	2819	2842	
$2^2D_{5/2}$	$\frac{5}{2}^+$	2771	2791	
$2^4D_{1/2}$	$\frac{1}{2}^+$	2874	2899	
$2^4D_{3/2}$	$\frac{3}{2}^+$	2838	2861	
$2^4D_{5/2}$	$\frac{5}{2}^+$	2790	2810	
$2^4D_{7/2}$	$\frac{7}{2}^+$	2729	2747	
$3^2D_{3/2}$	$\frac{3}{2}^+$	3455	3489	
$3^2D_{5/2}$	$\frac{5}{2}^+$	3391	3423	
$3^4D_{1/2}$	$\frac{1}{2}^+$	3527	3562	
$3^4D_{3/2}$	$\frac{3}{2}^+$	3479	3513	
$3^4D_{5/2}$	$\frac{5}{2}^+$	3415	3448	
$3^4D_{7/2}$	$\frac{7}{2}^+$	3336	3366	

Table 5. *F*-wave of Ξ baryon (in MeV).

State	J^P	$Mass_{\rm cal}1$	$Mass_{\rm cal}2$	$Mass_{\rm exp}$ [1]
$1^2F_{5/2}$	$\frac{5}{2}^-$	2713	2736	
$1^2F_{7/2}$	$\frac{7}{2}^-$	2647	2666	
$1^4F_{3/2}$	$\frac{3}{2}^-$	2786	2813	
$1^4F_{5/2}$	$\frac{5}{2}^-$	2733	2757	
$1^4F_{7/2}$	$\frac{7}{2}^-$	2667	2687	
$1^4F_{9/2}$	$\frac{9}{2}^-$	2588	2603	
$2^2F_{5/2}$	$\frac{5}{2}^-$	3333	3368	
$2^2F_{7/2}$	$\frac{7}{2}^-$	3249	3280	
$2^4F_{3/2}$	$\frac{3}{2}^-$	3426	3465	
$2^4F_{5/2}$	$\frac{5}{2}^-$	3358	3394	
$2^4F_{7/2}$	$\frac{7}{2}^-$	3274	3306	
$2^4F_{9/2}$	$\frac{9}{2}^-$	3173	3201	

Table 6. Comparison of masses with other predictions based on J^P value for Ξ baryon (in MeV).

J^P	$Mass_{\rm cal}1$	$Mass_{\rm cal}2$	[27]	[28]	[29]	[30]	[46]	[47]	[31]	[2]	[48]	[49]
$\frac{1}{2}^+$	1322	1321	1330	1310	1305	1334	1348	1317	1318	1325	1317	1303 ± 13
	1884	1891	1886	1876	1840	1727	1805	1772	1932	1891	1750	2178 ± 48
	2310	2322	1993	2062	2040	1932	1868				1980	2231 ± 44
	2361	2372	2012	2131	2100			1874			2054	2408 ± 45
	2874	2899	2091	2176	2130						2107	
	2935	2954	2142	2215	2150						2149	
	3527	3562	2367	2249	2230						2254	
	3591	3620			2345							
$\frac{3}{2}^+$	1531	1524	1518	1539	1505	1524	1528	1552	1539	1520	1526	1553 ± 18
	1971	1964	1966	1988	2045	1878		1653	2120	1934	1952	2228 ± 40
	2270	2281	2100	2076	2065	1979					1970	2398 ± 52
	2283	2295	2121	2128	2115						2065	2574 ± 52
	2457	2459	2122	2170	2165						2114	
	2819	2842	2144	2175	2170						2174	
	2838	2861	2149	2219	2210						2184	
	3029	3041	2421	2257	2230						2218	
	3455	3489		2279	2275						2252	
	3479	3513										
	3679	3702										
$\frac{5}{2}^+$	2234	2242	2108	2013	2045					1936	1959	
	2247	2295	2147	2141	2165					2025	2102	
	2771	2791	2213	2197	2230						2170	
	2790	2810		2231	2230						2205	
	3391	3423		2279	2240						2239	
	3415	3448										
$\frac{7}{2}^+$	2203	2211	2189	2169	2180					2035	2074	
	2729	2747		2289	2240						2189	
	3336	3366										

Table 7. Comparison of masses with other predictions based on J^P value forΞ baryon (in MeV).

J^P	$Mass_{\rm cal}1$	$Mass_{\rm cal}2$	[27]	[28]	[29]	[30]	[46]	[47]	[31]	[2]	[48]	[49]
$\frac{1}{2}^-$	1886	1889	1682	1770	1755	1869			1658	1725	1772	1716 ± 43
	1894	1897	1758	1922	1810	1932				1811	1894	1837 ± 28
	2361	2373	1839	1938	1835	2076					1926	1844 ± 43
	2373	2386	2160	2241	2225							2758 ± 78
	2929	2948	2210	2266	2285							
	2946	2966	2233	2387	2300							
	3577	3609	2261	2411	2320							
	3599	3632		2445	2380							

Continued on next page

Table 7-continued from previous page

J^P	$Mass_{\rm cal}1$	$Mass_{\rm cal}2$	[27]	[28]	[29]	[30]	[46]	[47]	[31]	[2]	[48]	[49]
$\frac{3}{2}^-$	1871	1873	1764	1780	1785	1828	1792	1861	1820	1759	1801	1906 ± 29
	1879	1881	1798	1873	1880	1869		1971		1826	1918	1894 ± 38
	2337	2347	1904	1924	1895	1932					1976	2497 ± 61
	2349	2360	2245	2246	2240							2426 ± 73
	2786	2813	2252	2284	2305							
	2894	2913	2350	2353	2330							
	2912	2931	2352	2384	2340							
	3426	3465		2416	2385							
	3532	3563										
	3554	3586										
$\frac{5}{2}^-$	1859	1859	1853	1955	1900	1881				1883	1917	
	2318	2325	2333	2292	2345							
	2713	2736	2411	2409	2350							
	2733	2757		2425	2385							
	2865	2884		2438								
	3333	3368										
	3358	3394										
	3494	3524										
$\frac{7}{2}^-$	2647	2666	2460	2320	2355							
	2667	2687	2474		2425							
	3249	3280		2464								
	3274	3306		2481								
$\frac{9}{2}^-$	2588	2603	2502	2505								
	3173	3201		2570								

Table 8. *S*-wave of Λ baryon (in MeV).

State	J^P	$Mass_{\rm cal}1$	$Mass_{\rm cal}2$	$Mass_{\rm exp}$ [1]
1*S*	$\frac{1}{2}^+$	1115	1115	1115
2*S*	$\frac{1}{2}^+$	1592	1589	1600
3*S*	$\frac{1}{2}^+$	1885	1892	1810
4*S*	$\frac{1}{2}^+$	2202	2220	
5*S*	$\frac{1}{2}^+$	2540	2571	

evidence for the states. Furthermore, the present calculations included masses up to 4 GeV.

Ref. [27] employed the relativistic quark-diquark model for the calculation of strange baryon mass spectra. As the model considers both ground and excited states of diquarks, the number of excited states is limited and confined to only lower states. Another relativistic approach based on the three quark Bethe-Salpeter equation with instantaneous two and three body forces is described by Ref. [28]. It introduced instanton induced hyperfine splitting of positive and negative parity states. A further approach is the well known relativised Capstick-Isgur model with higher order spin-dependent potential terms in a three quark system and has predicted masses for nearly 2 GeV [29].

The approach by R.Bijker *et al.* [30] uses an algebraic model. It is based on collective string-like qqq wherein the orbital excitations are treated as rotations and vibrations of the strings. Low-lying states are established by this model for octet and decuplet class but exact spin-parity are not assigned in the case of Ξ. Ref. [46] utilized the relativistic constituent quark model (RCQM) with Goldstone-boson exchange. Another relativistic quark-diquark approach with Coulomb plus linear interaction and an exchange term, which is inspired by Gürsey-Radicati, has been employed in Ref. [47] for low-lying resonance states

Table 9. P-wave of Λ baryon (in MeV).

State	J^P	$Mass_{\rm cal}1$	$Mass_{\rm cal}2$	$Mass_{\rm exp}$ [1]
$1^2P_{1/2}$	$\frac{1}{2}^-$	1546	1558	1670
$1^2P_{3/2}$	$\frac{3}{2}^-$	1534	1544	1520
$1^4P_{1/2}$	$\frac{1}{2}^-$	1553	1564	
$1^4P_{3/2}$	$\frac{3}{2}^-$	1540	1551	
$1^4P_{5/2}$	$\frac{5}{2}^-$	1524	1533	
$2^2P_{1/2}$	$\frac{1}{2}^-$	1834	1858	1800
$2^2P_{3/2}$	$\frac{3}{2}^-$	1819	1841	1690
$2^4P_{1/2}$	$\frac{1}{2}^-$	1841	1867	
$2^4P_{3/2}$	$\frac{3}{2}^-$	1827	1850	
$2^4P_{5/2}$	$\frac{5}{2}^-$	1807	1827	1830
$3^2P_{1/2}$	$\frac{1}{2}^-$	2149	2186	
$3^2P_{3/2}$	$\frac{3}{2}^-$	2131	2166	
$3^4P_{1/2}$	$\frac{1}{2}^-$	2158	2196	
$3^4P_{3/2}$	$\frac{3}{2}^-$	2140	2176	
$3^4P_{5/2}$	$\frac{5}{2}^-$	2116	2149	
$4^2P_{1/2}$	$\frac{1}{2}^-$	2484	2536	
$4^2P_{3/2}$	$\frac{3}{2}^-$	2464	2513	
$4^4P_{1/2}$	$\frac{1}{2}^-$	2495	2548	
$4^4P_{3/2}$	$\frac{3}{2}^-$	2474	2525	
$4^4P_{5/2}$	$\frac{5}{2}^-$	2447	2494	

Table 10. D-wave of Λ baryon (in MeV).

State	J^P	$Mass_{\rm cal}1$	$Mass_{\rm cal}2$	$Mass_{\rm exp}$ [1]
$1^2D_{3/2}$	$\frac{3}{2}^+$	1769	1789	1890
$1^2D_{5/2}$	$\frac{5}{2}^+$	1746	1767	1820
$1^4D_{1/2}$	$\frac{1}{2}^+$	1794	1814	
$1^4D_{3/2}$	$\frac{3}{2}^+$	1777	1798	
$1^4D_{5/2}$	$\frac{5}{2}^+$	1755	1776	
$1^4D_{7/2}$	$\frac{7}{2}^+$	1727	1748	
$2^2D_{3/2}$	$\frac{3}{2}^+$	2076	2113	2070
$2^2D_{5/2}$	$\frac{5}{2}^+$	2051	2085	2110

Continued on next page

Table 10-continued from previous page

State	J^P	$Mass_{\rm cal}1$	$Mass_{\rm cal}2$	$Mass_{\rm exp}$ [1]
$2^4D_{1/2}$	$\frac{1}{2}^+$	2105	2144	
$2^4D_{3/2}$	$\frac{3}{2}^+$	2086	2123	
$2^4D_{5/2}$	$\frac{5}{2}^+$	2060	2096	
$2^4D_{7/2}$	$\frac{7}{2}^+$	2029	2061	2085
$3^2D_{3/2}$	$\frac{3}{2}^+$	2408	2459	
$3^2D_{5/2}$	$\frac{5}{2}^+$	2378	2426	
$3^4D_{1/2}$	$\frac{1}{2}^+$	2441	2496	
$3^4D_{3/2}$	$\frac{3}{2}^+$	2419	2471	
$3^4D_{5/2}$	$\frac{5}{2}^+$	2389	2438	
$3^4D_{7/2}$	$\frac{7}{2}^+$	2352	2398	

Table 11. F-wave of Λ baryon (in MeV).

State	J^P	$Mass_{\rm cal}1$	$Mass_{\rm cal}2$	$Mass_{\rm exp}$ [1]
$1^2F_{5/2}$	$\frac{5}{2}^-$	2005	2039	
$1^2F_{7/2}$	$\frac{7}{2}^-$	1970	2002	2100
$1^4F_{3/2}$	$\frac{3}{2}^-$	2043	2079	
$1^4F_{5/2}$	$\frac{5}{2}^-$	2015	2050	
$1^4F_{7/2}$	$\frac{7}{2}^-$	1980	2013	
$1^4F_{9/2}$	$\frac{9}{2}^-$	1939	1969	
$2^2F_{5/2}$	$\frac{5}{2}^-$	2329	2380	
$2^2F_{7/2}$	$\frac{7}{2}^-$	2291	2337	
$2^4F_{3/2}$	$\frac{3}{2}^-$	2371	2427	
$2^4F_{5/2}$	$\frac{5}{2}^-$	2341	2393	
$2^4F_{7/2}$	$\frac{7}{2}^-$	2303	2350	
$2^4F_{9/2}$	$\frac{9}{2}^-$	2257	2299	
$3^2F_{5/2}$	$\frac{5}{2}^-$	2676	2741	
$3^2F_{7/2}$	$\frac{7}{2}^-$	2632	2693	
$3^4F_{3/2}$	$\frac{3}{2}^-$	2723	2793	
$3^4F_{5/2}$	$\frac{5}{2}^-$	2689	2755	
$3^4F_{7/2}$	$\frac{7}{2}^-$	2645	2707	
$3^4F_{9/2}$	$\frac{9}{2}^-$	2593	2650	

Table 12. G-wave of Λ baryon (in MeV).

State	J^P	$Mass_{\rm cal}1$	$Mass_{\rm cal}2$	$Mass_{\rm exp}$[1]
$1^2G_{7/2}$	$\frac{7}{2}^+$	2253	2302	
$1^2G_{9/2}$	$\frac{9}{2}^+$	2204	2246	2350
$1^4G_{5/2}$	$\frac{5}{2}^+$	2305	2363	
$1^4G_{7/2}$	$\frac{7}{2}^+$	2265	2316	
$1^4G_{9/2}$	$\frac{9}{2}^+$	2216	2260	
$1^4G_{11/2}$	$\frac{11}{2}^+$	2159	2195	

of Ξ. Y. Oh [31] has studied the cascade and omega baryons through a Skyrme model, which is based on the approximation of equal mass splitting of hyperon resonances. The mass formula is developed with isospin and spin in the soliton-kaon bound-state model. The Ξ has also been explored in large-N_c limits [52, 53] as well as through the QCD-SUM rule method [54]. M. Pervin [2] has obtained mass spectra using a non-relativistic quark model approach. Y. Chen *et al*. have implemented a different approach with a non-relativistic quark model supplemented with hyperfine interaction of a higher order $O(\alpha_s^2)$ [48]. Some low-lying states have been exploited

Table 13. Comparison of masses with other predictions based on J^P value for Λ baryon (in MeV).

J^P	$Mass_{\rm cal}1$	$Mass_{\rm cal}2$	[27]	[28]	[29]	[30]	[46]	[47]	[50]	[51]	[48]	[49]
$\frac{1}{2}^+$	1115	1115	1115	1108	1115	1133	1136	1116	1116	1112	1113	1149 ± 18
	1592	1589	1615	1677	1680	1577	1625	1518	1600	1695	1606	1807 ± 94
	1794	1814				1799	1799	1666	1810		1764	2112 ± 54
	1885	1892	1901	1747	1830			1955			1880	2137 ± 68
	2105	2144	1972	1898	1910			1960			2013	
	2202	2220	1986	2077	2010						2173	
	2441	2496	2042	2099	2105						2198	
	2540	2571	2099	2132	2120							
$\frac{3}{2}^+$	1769	1789	1854	1823	1900	1849		1896	1890	1903	1836	1991 ± 103
	1777	1798	1976	1952	1960				2000		1958	2058 ± 139
	2076	2113	2130	2045	1995					1993		2481 ± 111
	2086	2123	2184	2087	2050					2061		
	2408	2459	2202	2133	2080					2121		
	2419	2471									2134	
$\frac{5}{2}^+$	1746	1767	1825	1834	1890	1849		1896	1820	1846	1839	
	1755	1776	2098	1999	2035	2074			2110	2132	2008	
	2051	2085	2221	2078	2115						2103	
	2060	2096	2255	2127	2115						2129	
	2305	2363	2258	2150	2180						2155	
	2378	2426										
	2389	2471										
$\frac{7}{2}^+$	1727	1748	2251	2130	2120				2020		2064	
	2029	2061	2471	2331								
	2253	2302										
	2265	2316										
	2352	2398										
$\frac{9}{2}^+$	2204	2246	2360	2340		2357			2350	2360		
	2216	2260										
$\frac{11}{2}^+$	2159	2195							2585			

Table 14. Comparison of masses with other predictions based on J^P value for Λ baryon (in MeV).

J^P	$Mass_{\rm cal}1$	$Mass_{\rm cal}2$	[27]	[28]	[29]	[30]	[46]	[47]	[50]	[51]	[48]	[49]
$\frac{1}{2}^-$	1546	1558	1406	1524	1550	1686	1556	1650	1670	1679	1559	1416 ± 81
	1553	1564	1667	1630	1615	1799	1682	1732		1830	1656	1546 ± 110
	1834	1858	1733	1816	1675		1778	1969	1800		1791	1713 ± 116
	1841	1867	1927	2011	2015			1854				2075 ± 249
	2149	2186	2197	2076	2095			1928				
	2158	2196	2218	2117	2160							
	2484	2536										
	2495	2548										
$\frac{3}{2}^-$	1534	1544	1549	1508	1545	1686	1556	1650	1690	1683	1560	1751 ± 41
	1540	1551	1693	1662	1645		1682	1785	1520		1702	2203 ± 106
	1819	1841	1812	1775	1770			1854	2325		1859	2381 ± 87
	1827	1850	2035	1987	2030			1928				
	2043	2079	2319	2090	2110			1969				
	2131	2166	2322	2147	2185							
	2140	2176	2392	2259	2230							
	2371	2427	2454	2290	2275							
	2464	2513	2468	2313								
	2474	2525										
	2723	2793										
$\frac{5}{2}^-$	1524	1533										
	1807	1827	1861	1828	1775	1799	1778	1785	1830	1850	1803	
	2005	2039	2136	2080	2180							
	2015	2050	2350	2179	2250							
	2116	2149										
	2329	2380										
	2341	2393										
	2447	2494										
	2676	2741										
	2689	2755										
$\frac{7}{2}^-$	1970	2002	2097	2090	2150				2100	2087		
	1980	2013	2583	2227	2230							
	2291	2337										
	2303	2350										
	2632	2693										
	2645	2707										
$\frac{9}{2}^-$	1939	1969	2665	2370								
	2257	2299										
	2593	2650										

Table 15. *S*-wave of Σ baryon (in MeV).

State	J^P	$Mass_{\rm cal}1$	$Mass_{\rm cal}2$	$Mass_{\rm exp}$ [1]
$1S$	$\frac{1}{2}^+$	1193	1193	1193
	$\frac{3}{2}^+$	1384	1384	1385
$2S$	$\frac{1}{2}^+$	1643	1643	1660
	$\frac{3}{2}^+$	1827	1827	
$3S$	$\frac{1}{2}^+$	2083	2099	
	$\frac{3}{2}^+$	2229	2236	
$4S$	$\frac{1}{2}^+$	2560	2589	
	$\frac{3}{2}^+$	2675	2693	
$5S$	$\frac{1}{2}^+$	3067	3108	
	$\frac{3}{2}^+$	3159	3189	

Table 16. *P*-wave of Σ baryon (in MeV).

State	J^P	$Mass_{\rm cal}1$	$Mass_{\rm cal}2$	$Mass_{\rm exp}$ [1]
$1^2P_{1/2}$	$\frac{1}{2}^-$	1720	1725	1620
$1^2P_{3/2}$	$\frac{3}{2}^-$	1698	1702	1670
$1^4P_{1/2}$	$\frac{1}{2}^-$	1731	1736	1750
$1^4P_{3/2}$	$\frac{3}{2}^-$	1709	1713	
$1^4P_{5/2}$	$\frac{5}{2}^-$	1680	1683	1775
$2^2P_{1/2}$	$\frac{1}{2}^-$	2128	2145	1900
$2^2P_{3/2}$	$\frac{3}{2}^-$	2099	2114	1910
$2^4P_{1/2}$	$\frac{1}{2}^-$	2142	2159	
$2^4P_{3/2}$	$\frac{3}{2}^-$	2114	2129	
$2^4P_{5/2}$	$\frac{5}{2}^-$	2076	2087	
$3^2P_{1/2}$	$\frac{1}{2}^-$	2580	2608	
$3^2P_{3/2}$	$\frac{3}{2}^-$	2545	2571	
$3^4P_{1/2}$	$\frac{1}{2}^-$	2598	2627	
$3^4P_{3/2}$	$\frac{3}{2}^-$	2563	2589	
$3^4P_{5/2}$	$\frac{5}{2}^-$	2516	2541	
$4^2P_{1/2}$	$\frac{1}{2}^-$	3068	3111	
$4^2P_{3/2}$	$\frac{3}{2}^-$	3027	3067	
$4^4P_{1/2}$	$\frac{1}{2}^-$	3088	3133	
$4^4P_{3/2}$	$\frac{3}{2}^-$	3047	3089	
$4^4P_{5/2}$	$\frac{5}{2}^-$	2994	3030	
$5^2P_{1/2}$	$\frac{1}{2}^-$	3588	3641	
$5^2P_{3/2}$	$\frac{3}{2}^-$	3541	3594	
$5^4P_{1/2}$	$\frac{1}{2}^-$	3612	3664	
$5^4P_{3/2}$	$\frac{3}{2}^-$	3565	3617	
$5^4P_{5/2}$	$\frac{5}{2}^-$	3502	3555	

through dynamical chirally improved quarks by BGR Collaboration [49].

The ground state of Ξ has been very well established with known spin-parity at 1321 MeV and $J^P = \frac{1}{2}^+$ in the octet family. It is evident from Table 5 that the ground state fits well for nearly all the models owing to the minor variations in the assumptions of any given model. Another state is 1532 MeV with $J^P = \frac{3}{2}^+$ holding a place in decuplet. The mass for this state varies within 20 MeV among all the models discussed. The only negative parity state by PDG is 1823 MeV at $J^P = \frac{3}{2}^-$, which is obtained as 1871 MeV and 1879 MeV for octet and decuplet Ξ, respectively.

Ξ(1690) is a fairly well-known state in the PDG database; however, the spin-parity assignments and exact mass predictions vary considerably. The BABAR Collaboration concluded the state to be spin $\frac{1}{2}$ [6]. As shown in Table 6, various models have predicted this state in a comparatively higher mass from PDG, the nearest being 1682 MeV. Furthermore, due to the intrinsic drawback of the present model, a conclusive assignment of this state was not possible. The Ξ(2030) with assigned angular momentum value of $\frac{5}{2}$ is predicted here to be 2234 MeV with positive parity. Other model predictions vary within a 200 MeV range for the same spin-parity. Ξ(1620) appears in PDG with a one star status. Such a state is not established in this work, although one study shines light on the existence of Ξ(1620) and Ξ(1690) [55].

The PDG states Ξ(1950), Ξ(2250), and Ξ(2370) are three and two starred; however, due to lack of spin-parity assignment, the comparison is not reasonable. In addition, one study depicts the states of cascade around Ξ(1950) within the range of 1900-2000 MeV in three different states [56]. A few states in our results are comparatively near to those in the BGR work [49], which do not appear in other approaches.

For theΛ baryon, the ground state mass is 1115 MeV and for Σ it is 1193 MeV; the confinement parameters are determined accordingly. Here, the constituent quark masses for u and d quarks are similar; hence, the charges

Table 17. D-wave of Σ baryon (in MeV).

State	J^P	$Mass_{\rm cal}1$	$Mass_{\rm cal}2$	$Mass_{\rm exp}$ [1]
$1^2D_{3/2}$	$\frac{3}{2}^+$	2040	2057	1940
$1^2D_{5/2}$	$\frac{5}{2}^+$	1998	2013	1915
$1^4D_{1/2}$	$\frac{1}{2}^+$	2086	2107	
$1^4D_{3/2}$	$\frac{3}{2}^+$	2055	2074	
$1^4D_{5/2}$	$\frac{5}{2}^+$	2014	2029	
$1^4D_{7/2}$	$\frac{7}{2}^+$	1962	1974	2025
$2^2D_{3/2}$	$\frac{3}{2}^+$	2481	2510	
$2^2D_{5/2}$	$\frac{5}{2}^+$	2432	2459	
$2^4D_{1/2}$	$\frac{1}{2}^+$	2536	2568	
$2^4D_{3/2}$	$\frac{3}{2}^+$	2499	2529	
$2^4D_{5/2}$	$\frac{5}{2}^+$	2451	2478	
$2^4D_{7/2}$	$\frac{7}{2}^+$	2390	2414	
$3^2D_{3/2}$	$\frac{3}{2}^+$	2962	3004	
$3^2D_{5/2}$	$\frac{5}{2}^+$	2905	2945	
$3^4D_{1/2}$	$\frac{1}{2}^+$	3027	3072	
$3^4D_{3/2}$	$\frac{3}{2}^+$	2984	3027	
$3^4D_{5/2}$	$\frac{5}{2}^+$	2926	2967	
$3^4D_{7/2}$	$\frac{7}{2}^+$	2855	2892	
$4^2D_{3/2}$	$\frac{3}{2}^+$	3476	3534	
$4^2D_{5/2}$	$\frac{5}{2}^+$	3410	3464	
$4^4D_{1/2}$	$\frac{1}{2}^+$	3549	3613	
$4^4D_{3/2}$	$\frac{3}{2}^+$	3500	3560	
$4^4D_{5/2}$	$\frac{5}{2}^+$	3435	3490	
$4^4D_{7/2}$	$\frac{7}{2}^+$	3353	3403	

Table 18. F-wave of Σ baryon (in MeV).

State	J^P	$Mass_{\rm cal}1$	$Mass_{\rm cal}2$	$Mass_{\rm exp}$ [1]
$1^2F_{5/2}$	$\frac{5}{2}^-$	2386	2416	
$1^2F_{7/2}$	$\frac{7}{2}^-$	2318	2343	
$1^4F_{3/2}$	$\frac{3}{2}^-$	2461	2495	
$1^4F_{5/2}$	$\frac{5}{2}^-$	2406	2437	
$1^4F_{7/2}$	$\frac{7}{2}^-$	2338	2365	
$1^4F_{9/2}$	$\frac{9}{2}^-$	2257	2278	
$2^2F_{5/2}$	$\frac{5}{2}^-$	2858	2901	
$2^2F_{7/2}$	$\frac{7}{2}^-$	2781	2819	
$2^4F_{3/2}$	$\frac{3}{2}^-$	2943	2990	
$2^4F_{5/2}$	$\frac{5}{2}^-$	2881	2925	
$2^4F_{7/2}$	$\frac{7}{2}^-$	2804	2844	
$2^4F_{9/2}$	$\frac{9}{2}^-$	2712	2746	
$3^2F_{5/2}$	$\frac{5}{2}^-$	3363	3417	
$3^2F_{7/2}$	$\frac{7}{2}^-$	3278	3330	
$3^4F_{3/2}$	$\frac{3}{2}^-$	3456	3512	
$3^4F_{5/2}$	$\frac{5}{2}^-$	3388	3443	
$3^4F_{7/2}$	$\frac{7}{2}^-$	3303	3356	
$3^4F_{9/2}$	$\frac{9}{2}^-$	3202	3252	

of Σ are not distinguished. The four star status states are in good agreement with the PDG masses, as evident from the tables. As for the excited states of Λ 2S(1600), the predicted masses are very near to almost all the model masses. However, the first negative parity state Λ(1405) $J^P=\frac{1}{2}^-$ is not established by the present model, and the next state with $J^P=\frac{3}{2}^-$ 1520 MeV varies by 15 MeV from that in PDG. The $J^P=\frac{5}{2}^+$ state of 1D (1769 MeV) also falls within the PDG mass range of 1750-1850. The $J^P=\frac{9}{2}^+$ for 1G is somewhat under-predicted owing to the limitations of the hCQM.

For the case of the Σ baryon, the early negative parity states are just one star status. The later state with $J^P=\frac{1}{2}^-$ appearing as Σ(1750) is predicted well here as 1720 MeV within the range 1700-1800. The $J^P=\frac{5}{2}^+$ Σ(1915) is slightly higher, predicted from most of the models. The results of the other higher ranged states from hCQM are comparable to those of the BGR Collaboration [49].

IV. REGGE TRAJECTORIES

Regge trajectories have been one of the most useful tools in spectroscopic studies. The plots of total angular momentum, J, and principal quantum number, n, against the square of resonance mass, M^2, are drawn based on calculated data. The non-intersecting and linearly fitted lines were in accordance with theoretical and experiment-

Table 19. Comparison of masses with other predictions based on J^P value for Σ baryon (in MeV).

J^P	$Mass_{cal}1$	$Mass_{cal}2$	[27]	[28]	[29]	[30]	[46]	[47]	[50]	[51]	[48]	[49]
$\frac{1}{2}^+$	1193	1193	1187	1190	1190	1170	1180	1211	1193	1198	1192	1216 ± 15
	1643	1643	1711	1760	1720	1604	1616	1546	1660	1656	1664	2069 ± 74
	2083	2099	1922	1947	1915		1911	1668	1770		1924	2149 ± 66
	2086	2107	1983	2009	1970			1801	1880		1986	2335 ± 63
	2536	2568	2028	2052	2005						2022	
	2560	2589	2180	2098	2030						2069	
	3027	3072	2292	2138	2105						2172	
	3067	3108	2472									
	3549	3613										
$\frac{3}{2}^+$	1384	1384	1381	1411	1370	1382	1389	1334	1385	1381	1383	1471 ± 23
	1827	1827	1862	1896	1920		1865	1439	1560		1868	2194 ± 81
	2040	2057	2025	1961	1970			1924	1690		1947	2250 ± 79
	2055	2074	2076	2011	2010				1840		1993	2468 ± 67
	2229	2236	2096	2044	2030						2039	
	2481	2510	2157	2062	2045						2075	
	2499	2529	2186	2103	2085						2098	
	2675	2693		2112	2115						2122	
	2962	3004									2168	
	2984	3027										
	3159	3189										
$\frac{5}{2}^+$	1998	2013	1991	1956	1995	1872		2061	1915	1930	1949	
	2014	2029	2062	2027	2030				2070		2028	
	2432	2459	2221	2071	2095						2062	
	2451	2478									2107	
	2905	2945									2154	
	2926	2967										
	3410	3464										
	3435	3490										
$\frac{7}{2}^+$	1962	1974	2033	2070	2060	2012			2030	2039	2002	
	2390	2414	2470	2161	2125						2106	
	2855	2892										
	3353	3403										

al data in many studies [57]. These plots might be helpful in predicting the correct spin-parity assignment of a given state.

$$J = aM^2 + a_0, \tag{9}$$

$$n = bM^2 + b_0. \tag{10}$$

As is evident from Figs. 1-3, the Regge trajectory for n against M^2 has been linearly fitted for the calculated resonance masses, which follow the expected trend. The trajectories for J against M^2 for the natural parity as depicted in Figs. 4-8 also follow the linear nature, which signifies that the spin-parity assignment for the obtained states are in agreement. The overall nature of the Regge trajectories observed in baryon studies agrees with the calculated results for a few of the states.

Table 20. Comparison of masses with other predictions based on J^P value for Ξ baryon (in MeV).

J^P	$Mass_{\rm cal}1$	$Mass_{\rm cal}2$	[27]	[28]	[29]	[30]	[46]	[47]	[50]	[51]	[48]	[49]
$\frac{1}{2}^-$	1720	1725	1620	1628	1630	1711	1677	1753	1620	1754	1657	1603 ± 38
	1731	1736	1693	1771	1675		1736	1868	1750		1746	1718 ± 58
	2128	2145	1747	1798	1695		1759	1895	2000		1802	1730 ± 34
	2142	2159	2115	2111	2110							2478 ± 104
	2580	2608	2198	2136	2155							
	2598	2627	2202	2251	2165							
	3068	3111	2289	2264	2205							
	3088	3133	2381	2288	2260							
	3588	3641										
	3612	3664										
$\frac{3}{2}^-$	1698	1702	1706	1669	1655	1711	1677	1753	1670	1697	1698	1861 ± 26
	1709	1713	1731	1728	1750	1974	1736	1868	1940	1956	1790	1736 ± 40
	2099	2114	1856	1781	1755		1759	1895	2250		1802	2394 ± 74
	2114	2129	2175	2139	2120							2297 ± 122
	2416	2495	2203	2171	2185							
	2545	2571	2300	2203	2200							
	2563	2589										
	2943	2990										
	3027	3067										
	3047	3089										
	3456	3512										
	3541	3594										
	3565	3617										
$\frac{5}{2}^-$	1680	1683	1757	1770	1755		1736	1753	1775	1777	1743	
	2076	2087	2214	2174	2205							
	2386	2416	2347	2226	2250							
	2406	2437										
	2516	2541										
	2858	2901										
	2881	2925										
	2994	3030										
	3363	3417										
	3388	3443										
	3565	3617										
$\frac{7}{2}^-$	2318	2343	2259	2236	2245				2100			
	2338	2365	2349	2285								
	2781	2819										
	2804	2844										
	3278	3330										
	3303	3356										
$\frac{9}{2}^-$	2257	2278	2289	2325								
	2712	2746										
	3202	3252										

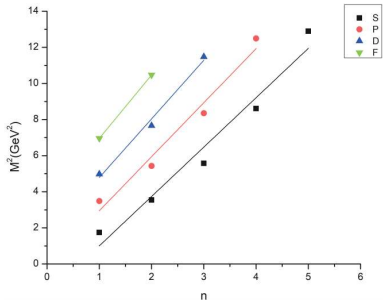

Fig. 1. (color online) Regge trajectory Ξ for $n \to M^2$

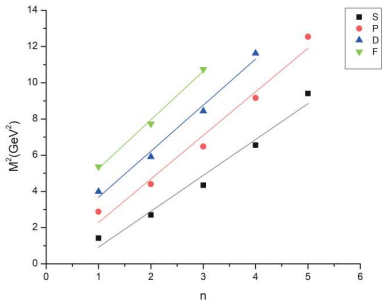

Fig. 2. (color online) Regge trajectory Σ for $n \to M^2$

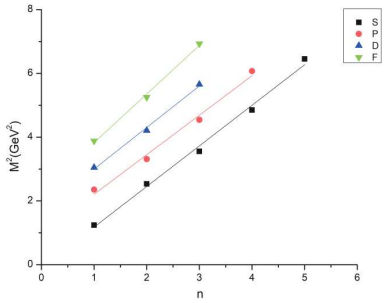

Fig. 3. (color online) Regge trajectory Λ for $n \to M^2$

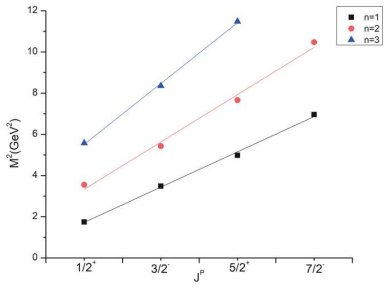

Fig. 4. (color online) Regge trajectory Ξ for $J^P \to M^2$

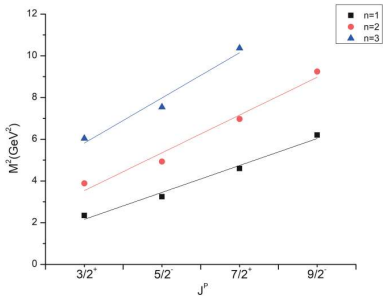

Fig. 5. (color online) Regge trajectory Ξ for $J^P \to M^2$

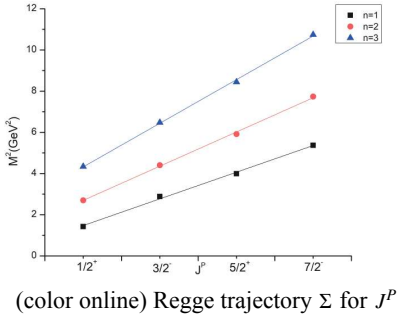

Fig. 6. (color online) Regge trajectory Σ for $J^P \to M^2$

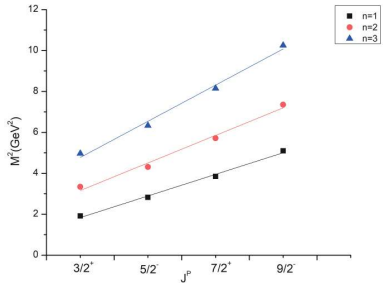

Fig. 7. (color online) Regge trajectory Σ for $J^P \to M^2$

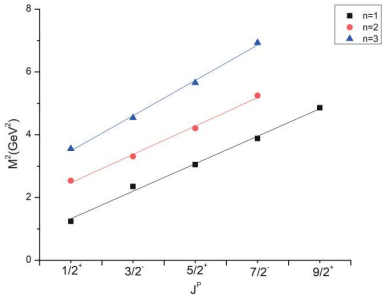

Fig. 8. (color online) Regge trajectory Λ for $J^P \to M^2$

V. MAGNETIC MOMENT

The study of electromagnetic properties of baryons is an active area for theoretical as well as experimental work. This intrinsic property helps reveal the shape and other dynamics of transition in decay modes. In the case of cascade Ξ and Σ baryon, the magnetic moment is to be determined for both spin configurations based on the respective spin-flavor wave-function. The generalized form of the magnetic moment is

$$\mu_B = \sum_q \left\langle \phi_{\rm sf} | \mu_{qz} | \phi_{\rm sf} \right\rangle, \tag{11}$$

where $\phi_{\rm sf}$ is the spin-flavor wave function. The contribution from an individual quark appears as

$$\mu_{qz} = \frac{e_q}{2m_q^{\rm eff}} \sigma_{qz}, \tag{12}$$

e_q being the quark charge, σ_{qz} being the spin orientation, and $m_q^{\rm eff}$ is the effective mass, which may vary from model-based quark mass due to the interactions. Here, is it noteworthy that a magnetic moment shall have contributions from many other effects within the baryon such as the sea quark, valence quark, and orbital. Various models have contributed to obtaining the magnetic moment of the octet and decuplet baryons. The order of quarks in spin-flavor will not affect the magnetic moment calculation. The final spin-flavor wave function along with the calculated ground state magnetic moment in terms of the nuclear magneton (μ_N) are mentioned in Table 21.

Table 22 provides a comparison of present magnetic moments with those of different approaches. H. Dahiya *et al*. presented octet and decuplet baryon magnetic moments in a chiral quark model with configuration mixing and generalizing the Cheng-Li mechanism. Effective mass and a screened charge scheme have been employed in Refs. [62], and both results appear in the table. Light-cone sum rules [63] and lattice QCD [64] have also been employed for octet and decuplet magnetic moments. A recent study focused on the hyperonic medium at a finite temperature using the chiral mean field approach [65]. Our results are under-predicted compared to the experimental values of PDG by 0.5 and 0.4 for Ξ octet baryons; however, there are large variations in the case of decuplet considering all the approaches. It is expected that experimental decuplet values shall be the deciding factor. In the case of Λ^0, the magnetic moment is nearly the same as those obtained in [1], [58], and [64]. For Σ^+ and Σ^-, the results are within a $0.5\mu_N$ variation for all the approaches.

Table 21. Magnetic moment for ground states.

Spin	Baryon	σ_{qz}	*Mass*/MeV	μ (μ_N)
$\frac{1}{2}$	Ξ^0(uss)	$\frac{1}{3}(4\mu_s-\mu_u)$	1322	−1.50
$\frac{1}{2}$	Ξ^-(dss)	$\frac{1}{3}(4\mu_s-\mu_d)$	1322	−0.46
$\frac{3}{2}$	Ξ^{*0}(uss)	$(2\mu_s+\mu_u)$	1531	0.766
$\frac{3}{2}$	Ξ^{*-}(dss)	$(2\mu_s+\mu_d)$	1531	−1.962
$\frac{1}{2}$	Σ^+(uus)	$\frac{1}{3}(4\mu_u-\mu_s)$	1193	2.79
$\frac{1}{2}$	Σ^0(uds)	$\frac{1}{3}(2\mu_u+2\mu_d-\mu_s)$	1193	0.839
$\frac{1}{2}$	Σ^-(dds)	$\frac{1}{3}(4\mu_d-\mu_s)$	1193	−1.113
$\frac{3}{2}$	Σ^{*+}(uus)	$(2\mu_u+\mu_s)$	1384	2.877
$\frac{3}{2}$	Σ^{*0}(uds)	$(\mu_u+\mu_d+\mu_s)$	1384	0.353
$\frac{3}{2}$	Σ^{*-}(dds)	$(2\mu_d+\mu_s)$	1384	−2.171
$\frac{1}{2}$	Λ^0(uds)	μ_s	1115	−0.606

Here, an effort has been made to determine the magnetic moment of the low-lying negative parity state of Ξ, which was inspired by studies based on $N(1535)$. The hyperfine interactions between the constituent quarks induce linear combinations of two states with the same angular momentum value. The magnetic moment will now have contribution from spin as well as orbital angular momentum as [67]

$$\mu=\mu^S+\mu^L=\sum\frac{Q_q}{m_q}S_q+\sum\frac{Q_q}{2m_q}l_q. \tag{13}$$

The $J^P=\frac{1}{2}^-$, $L=1$ for $S=\frac{1}{2}$ and $S=\frac{3}{2}$, and calculated resonance masses are 1886 and 1894 MeV, respectively. These states are not experimentally established; however, 1690 MeV is tentatively assigned by many predictions to this state. The physical eigenvalues will be

Table 22. Comparison of calculated magnetic moments with various models (All data in units of μ_N).

Baryon	$\mu_{\rm cal}$	Exp [1]	[58]	[58]	[59]	[60, 61]	[62]	[62]	[63]	[64]	[65]	[66]
Ξ^0	−1.50	−1.25	−1.41	−1.39		−1.3			−1.25	−1.37		
Ξ^-	−0.46	−0.651	−0.50	−0.50		−0.7			−1.07	−0.82		
Ξ^{*0}	0.766		0.60	0.49	0.49	0.69	0.48	0.32	0.44	0.16	0.508	0.65
Ξ^{*-}	−1.962		−2.11	−2.43	−2.27	−1.18	−1.9	−2.05	−2.27	−0.62	−1.805	−2.30
Σ^+	2.79	2.458	2.61	2.64					2.46	2.87		
Σ^0	0.839					0.11			0.65	0.76		
Σ^-	−1.113	−1.16	−1.01	−1.28		−1.13			−1.16	−1.48		
Σ^{*+}	2.877		3.02	3.07	2.85		2.56	2.54	2.63	1.27	3.028	
Σ^{*0}	0.353		0.30	0.08	0.09		0.23	0.14	0.08	0.33	0.188	
Σ^{*-}	−2.171		−2.41	−2.92	−2.66		−2.10	−2.19	−2.43	−1.88	−2.015	
Λ^0	−0.606	−0.613	−0.59	−0.60		−0.11			−0.51	−0.70		

$$|\Xi(1886)\rangle = \cos\theta|^2P_{1/2}\rangle - \sin\theta|^4P_{1/2}\rangle, \tag{14}$$

$$|\Xi(1894)\rangle = \sin\theta|^2P_{1/2}\rangle + \cos\theta|^4P_{1/2}\rangle. \tag{15}$$

From the approach of NCQM described in Ref. [68], we directly write the final wave-function with mixing for $\Xi^0(uss)$ as

$$\left(\frac{2}{9}\mu_s + \frac{1}{9}\mu_u\right)\cos^2\theta + \left(\mu_s + \frac{1}{3}\mu_u\right)\sin^2\theta - \left(\frac{8}{9}\mu_s - \frac{8}{9}\mu_u\right)\cos\theta\sin\theta. \tag{16}$$

The mixing angle is taken as $\theta = -31.7$. The magnetic moment for $\Xi^0(1886)$ is obtained to be -0.695μ_N, which is -0.99μ_N by [68]. Similarly, for $\Xi^-(1886)$, the magnetic moment is obtained as -0.193μ_N as compared to -0.315μ_N [68]. The variation relies on the fact that resonance mass is model dependent and the effective mass used in the calculation ultimately depends on resonance mass.

VI. TRANSITION MAGNETIC MOMENT AND RADIATIVE DECAY WIDTH

The transition magnetic moment as well as the radiative decay width are important in the understanding of the internal structure of baryon in addition to the magnetic and electric transitions. Many approaches have been used for the study of radiative decay over the years including some recent ones [69]. Here, $\Xi^{*0} \to \Xi^0\gamma$ and $\Sigma^* \to \Sigma\gamma$ have been studied using the effective mass obtained with the hCQM approach. The generalized form for the transition magnetic moment is [70],

$$\mu(B_{\frac{3}{2}^+} \to B_{\frac{1}{2}^+}) = \langle B_{\frac{1}{2}^+}, S_z = \frac{1}{2}|\mu_z|B_{\frac{3}{2}^+}, S_z = \frac{1}{2}\rangle. \tag{17}$$

The spin-flavor wave function is obtained similar to the above for decuplet and octet Ξ as

$$\frac{2\sqrt{2}}{3}(\mu_u^{\rm eff} - \mu_s^{\rm eff}). \tag{18}$$

The effective mass here is a geometric mean of those for spin $\frac{1}{2}$ and $\frac{3}{2}$. Our result comes out to be 2.378μ_N, which is in good agreement with various models implemented in [62, 70]. The radiative decay width is obtained as [71]

$$\Gamma_R = \frac{q^3}{m_p^2}\frac{2}{2J+1}\frac{e^2}{4\pi}\left|\mu_{\frac{3}{2}^+\to\frac{1}{2}^+}\right|^2, \tag{19}$$

where q is the photon energy, m_p is the proton mass, and J is the initial angular momentum giving Γ_R = 0.214 MeV. The total decay width available from the experiment is 9.1 MeV. Thus, the branching ratio $\frac{\Gamma_R}{\Gamma_{\rm total}}$ is 2.35%, where the PDG data suggests < 3.7%. Thus, it is in accordance with other results as well as the experimental data. The radiative decay of Σ baryons with transition magnetic moments are summarized in Table 23. The obtained results are consistent with experimental data from PDG as well as a few other theoretical approaches.

Table 23. Σ^* Radiative decays.

Decay	Wave-function	Transition moment(in μ_N)	Γ_R(in MeV)
$\Sigma^{*0} \to \Lambda^0\gamma$	$\frac{\sqrt{2}}{\sqrt{3}}(\mu_u - \mu_d)$	2.296	0.4256
$\Sigma^{*0} \to \Sigma^0\gamma$	$\frac{\sqrt{2}}{3}(\mu_u + \mu_d - 2\mu_s)$	0.923	0.0246
$\Sigma^{*+} \to \Sigma^+\gamma$	$\frac{2\sqrt{2}}{3}(\mu_u - \mu_s)$	2.204	0.1404
$\Sigma^{*-} \to \Sigma^-\gamma$	$\frac{2\sqrt{2}}{3}(\mu_d - \mu_s)$	−0.359	0.0037

VII. CONCLUSION

The present work aimed at studying the strangeness of -1 Λ and Σ and -2 Ξ light baryon owing to the limited data on these. The non-relativistic hypercentral constituent quark model (hCQM) has been a tool for obtaining a large number of resonance masses with a linear term. The results have been compared for cases with and without first order correction terms as well, where there is a difference of a few MeV for low-lying states and up to 30 MeV for higher excited states for Ξ. The octet and decuplet states have not been exclusively distinguished due to a lack of required data.

The mass-range has been compared to various theoretical approaches listed in Sec. 3. The state-wise comparison is not possible because no approach has established spin-parity assignments. The overview of Tables 6 and 7 shows that the low-lying resonance masses are in good agreement among each other especially the four star states of PDG. For higher excited states, present work overestimates the results compared to other models. The $\Xi(1820)$ differs by 48 MeV from the PDG mass. The $\Xi(2030)$ state with $J = \frac{5}{2}$ could find a place with either positive or negative parity as both have masses in that range. $\Xi(1620)$ and $\Xi(1690)$ are not obtained in present results. However, $\Xi(1690)$, which is likely $\frac{1}{2}^-$ as found by BABAR Collaboration, is calculated as 1886 MeV in this work. A few differences in results exist owing to the model dependent factors. As for $\Lambda(1405)$, hCQM could not establish the mass but predicts the other negative parity state with good agreement. The four star states for Σ and Λ also agree with many approaches to a good extent.

The Regge trajectories based on some resonance mass are plotted. The principal quantum number n against the square of mass M^2 shows a linear nature but the fitted lines are not exactly parallel. The angular momentum J versus the square of mass M^2 plots also depict the linearity of data points, which validates our spin-parity assignments to a particular state and may be helpful in new experimental states.

The magnetic moments for spin $\frac{1}{2}$ as well as Ξ^0 and Ξ^- vary by $0.25\mu_N$ and $0.19\mu_N$, respectively, from those of PDG as well as other results. For spin $\frac{3}{2}$ as well as Ξ^{*0} and Ξ^{*-}, our results vary from nearly $0.2\mu_N$ to $0.4\mu_N$ compared to all approaches. The transition magnetic moment is obtained for Ξ^0 1886 MeV of our spectra, which differs by $0.30\mu_N$, and Ξ^- differs by $0.12\mu_N$ from that in Ref. [68]. However, the difference in magnetic moment follows due to the difference in resonance masses used for the calculation. Similarly for Σ^+, Σ^-, and Λ^0, the results are in good accordance with other approaches and PDG.

The transition magnetic moment was obtained as $2.378\mu_N$, which agrees with other models. Moreover, the radiative decay width branching fraction was found to be 2.35% in our case, which was well within the PDG range of $< 3.7\%$. The transition magnetic moment and radiative decay width for Σwere similar to other results.

Thus, with some agreements and discrepancies, this work with a large number of predicted resonances along with important properties, may be helpful for upcoming experimental facilities like PANDA, which is expected to intensively study the light strange baryons [10-13, 15, 16].

ACKNOWLEDGEMENT

Ms. Chandni Menapara would like to acknowledge the support from the Department of Science and Technology (DST) under the INSPIRE-FELLOWSHIP scheme for pursuing this work.

References

[1] P. A. Zyla *et al.* (Particle Data Group), Prog. Theor. Exp. Phys. **2020**, 083C01 (2020)
[2] M. Pervin and W. Roberts, Phys. Rev. C **77**, 025202 (2008)
[3] S. Acharya *et al.* (ALICE Collaboration), Phys. Rev. Lett. **123**, 112002 (2019), arXiv:1904.12198[nucl-ex]
[4] E. Abouzaid *et al.* (KTeV Collaboration), Phys. Rev. Lett. **95**, 081801 (2005)
[5] J. R. Batley *et al.* (NA48/I Collaboration), Phys. Lett. B **645**, 36 (2007)
[6] B. Aubert *et al.* (BABAR Collaboration), Phys. Rev. Lett. **97**, 112001 (2006)
[7] W. Price *et al.* (CLAS Collaboration), Phys. Rev. C **71**, 058201 (2005)
[8] M. Amaryam *et al.* (KLF Collaboration), arXiv: 2008.08215 [nucl-ex] (2020)
[9] M. Ablikim *et al.* (BESIII Collaboration), Phys. Rev. D **100**, 051101(R) (2019)
[10] B. Singh *et al.* (PANDA Collaboration), J. Phys. G: Nucl. Part. Phys. **46**, 045001 (2019)
[11] B. Singh *et al.* (PANDA Collaboration), Phys. Rev. D **95**(3), 032003 (2017)
[12] B. Singh *et al.* (PANDA Collaboration), Eur. Phys. J. A **52**(10), 325 (2016)
[13] B. Singh *et al.* (PANDA Collaboration), Eur. Phys. J. A **51**, 107 (2015)
[14] J. Pütz *et al.* (PANDA Collaboration), EPJ Web Conf. **241**, 03004 (2020)
[15] G. Barruca *et al.* (PANDA Collaboration), Eur. Phys. J. A **57**(1), 30 (2021)
[16] G. Barruca *et al.* (PANDA Collaboration), Eur. Phys. J. A **55**, 42 (2019); arXiv:2009.11582; arXiv:2101.11877; arXiv: 2012.01776
[17] M. Mai, arXiv: 2010.00056
[18] D. Jido, J. A. Oller, E. Oset *et al.*, Nucl. Phys. A **725**, 181 (2003)
[19] C. Fernandez-Ramirez, I. V. Danilkin, D. M. Manley *et al.*, Phys. Rev. D **93**(3), 034029 (2016)
[20] H. Kamano, S. X. Nakamura, T.-S.H. Lee *et al.*, Phys. Rev. C **90**(6), 065204 (2014)
[21] Xiu-Lei Ren, E. Epelbaum, J. Gegelia *et al.*, arXiv: 2102.00914v1 (2021)
[22] E. Klempt *et al.* (Baryon@PDG Group), Eur. Phys. J. A **56**, 261 (2020)
[23] Sang-Ho Kim, K. P. Khemchandani, A. Martínez Torres *et al.*, arXiv: 2101.08668v1 (2021)
[24] J. K. Ahn and Seung-il Nam, arXiv: 2101.10114v1 (2021)
[25] T. hyodo and M. Niiyama, arXiv: 2010.07592[hep-ph] (2020)
[26] Li-Ye Xiao and Xian-Hui Zhong, Phys. Rev. D **87**, 094002 (2013)
[27] R. N. Faustov and V. O. Galkin, Phys. Rev. D **92**, 054005 (2015)
[28] U. Löring, B. Ch. Metsch, and H. R. Petry, Eur. Phys. J. A. **10**, 447-486 (2001)
[29] S. Capstick and N. Isgur, Phys. Rev. D **34**, 2809 (1986)
[30] R. Bijker, F. Iachello, and A. Leviatan, Ann. Phys. (N.Y.) **284**, 89-113 (2000)
[31] Y. Oh, Phys. Rev. D **75**, 074002 (2007)
[32] M. M. Giannini and E. Santopinto, Chin. J. Phys. **53**, 020301 (2015)
[33] C. Menapara, Z. Shah, and A. K. Rai, Chin. Phys. C **45**, 023102 (2021)
[34] C. Menapara, Z. Shah, and A. K. Rai, AIP Conf.Proc. **2220**, 140014 (2020)
[35] C. Menapara, Z. Shah, and A. K. Rai, Proc. of the DAE Symp. on Nucl. Phys. **64**, 673 (2019)
[36] Z. Shah, K. Gandhi, and A. K. Rai, Chin. Phys. C **43**, 034102 (2019), arXiv:1812.04858[hep-ph]
[37] B. Patel, A. K. Rai, and P. C. Vinodkumar, J. Phys. G: Nucl. Part. Phys **3**(6), 065001 (2008)
[38] B. Patel, A. K. Rai, and P. C. Vinodkumar, Pramana **66**, 953 (2006)

[39] M. Ferraris, M. M. Giannini, M. Pizzo *et al*., Phys. Lett. B. **364**, 231-238 (1995)
[40] M. M. Giannini, E. Santopinto, and A. Vassallo, Eur. Phys. J. A. **12**, 447-452 (2001)
[41] M. B. Voloshin, Prog. Part. Nucl. Phys. **61**, 455-511 (2008), arXiv:0711.4556
[42] Z. Shah and A. K. Rai, Eur. Phys. J. C **77**, 129 (2017)
[43] Z. Shah and A. K. Rai, FewBody Syst. **59**, 112 (2018)
[44] Z. Shah and A. K. Rai, Few-Body Syst. **59**, 76 (2018)
[45] W. Lucha and F. schoberls, Int. J. Modern Phys. C. **10**, 607 (1997)
[46] T. Melde, W. Plessas, and B. Sengl, Phys. Rev. D **77**, 114002 (2008)
[47] E. Santopinto and J. Ferretti, Phys. Rev. C **92**(2), 025202 (2015)
[48] Y. Chen and Bo-Qiang Ma, Nucl. Phys. A **831**, 1-21 (2009)
[49] G. P. Engel *et al*. (BGR Collaboration), Phys. Rev. D **87**, 074504 (2013)
[50] N. Matagne and Fl. Stancu, Phys. Rev. D **74**, 034014 (2006)
[51] J. L. Goity, C. L. Schat, and N. N. Scoccola, Phys. Rev. D **66**, -114014 (2002)
[52] F. X. Lee and X. Liu, Phys. Rev. D. **66**, 014014 (2002)
[53] Y. Chen and Bo-Qiang Ma, Chin. Phys. Lett. **25**, 3920 (2008)
[54] N. Amiri, M. Ghapanvari, and M. A. Jafarizadeh, Eur. Phys. J. Plus **136**, 141 (2021)
[55] A. Ramos, E. Oset, and C. Bennhold, Phys. Rev. Lett. **89**, 252001 (2002)
[56] M. Pavón Valderrama, Ju-Jun Xie, and J. Nieves, Phys. Rev. D **85**, 017502 (2012)
[57] Z. Shah, K. Thakkar, and A. K. Rai, Eur. Phys. J. C **76**, 530 (2016)
[58] H. Dahiya and M. Gupta, Phys. Rev. D **67**, 114015 (2003)
[59] J. Linde, T. Ohlsson, and H. Snellman, Phys. Rev. D **57**, 5916-5919 (1998)
[60] T. M. Aliev and V. S. Zamiralov, Adv. High Energy Phys. **2015**, 406875 (2015)
[61] T. M. Aliev, A. Özpineci, and M. Savci, Phys. Rev. D **66**, 016002 (2002)
[62] R. Dhir and R. C. Verma, Eur. Phys. J. A **42**, 243 (2009)
[63] S. Hong, Phys. Rev. D **76**, 094029 (2007)
[64] F. X. Lee, R. Kelly, L. Zhou *et al*., Phys. Lett. B **627**, 71 (2005)
[65] H. Singh, A. Kumar, and H. Dahiya, Eur. Phys. J. Plus **135**, 422 (2020)
[66] A. J. Buchmann, J. A. Hester, and R. F. Lebed, Phys. Rev. D **66**, 056002 (2002)
[67] J. Liu, J. He, and Y. B. Dong, Phys. rev. D **71**, 094004 (2005)
[68] N. Sharma, A. Martinez Torres, K. P. Khemchandani *et al*., Eur. Phys. J. A **49**, 11 (2013)
[69] Fayyazuddin and M. J. Aslam, arXiv: 2011.06750[hep-ph] (2020)
[70] H. Dahiya, Chin. Phys. C **42**(9), 093102 (2018)
[71] K. Thakkar, B. Patel, A. Majethiya *et al*., PRAMANA J of Physics **77**, 1053-1067 (2011)